

**The Effect of Welding Parameters Between Titanium Alloy and Stainless Steel
with Interlayer of Aluminium Alloy in Resistance Spot Welding**

by

Gan Yee Chuok

22691

Dissertation submitted in partial fulfilment of
the requirements for the
Bachelor of Mechanical Engineering
With Honours

JANUARY 2020

Universiti Teknologi PETRONAS
32610 Seri Iskandar
Perak Darul Ridzuan

CERTIFICATION OF APPROVAL

The Effect of Welding Parameters between Titanium Alloy and Stainless Steel with Interlayer of Aluminium Alloy in Resistance Spot Welding

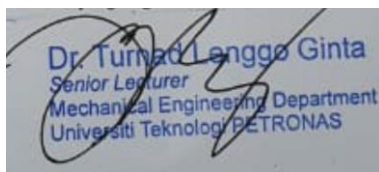
by

Gan Yee Chuok

22691

A project dissertation submitted to the
Mechanical Engineering Programme
Universiti Teknologi PETRONAS
in partial fulfilment of the requirement for the
BACHELOR OF MECHANICAL ENGINEERING
WITH HONOURS

Approved by,

A rectangular stamp containing a handwritten signature in blue ink over a printed name and title. The printed text reads: "Dr. Turnad Lenggo Ginta", "Senior Lecturer", "Mechanical Engineering Department", and "Universiti Teknologi PETRONAS".

(Dr. Turnad Lenggo Ginta)

UNIVERSITI TEKNOLOGI PETRONAS

BANDAR SERI ISKANDAR, PERAK

January 2020

CERTIFICATION OF ORIGINALITY

This is to certify that I am responsible for the work submitted in this project, that the original work is my own except as specified in the references and acknowledgements, and that the original work contained herein have not been undertaken or done by unspecified sources or persons.

Derick Gan

GAN YEE CHUOK

ABSTRACT

Resistance spot welding is a common fabrication method used in industry today. This manufacturing process always used for industry today because it is low cost, fast, and convenient in the assembly line. To obtain optimum condition during welding, proper setting of welding parameters such as weld current, electrode force, and weld time are needed. The main reason is welding input parameters affect the weld joint quality of specimens and thus give direct impact to mechanical properties of materials in term of tensile strength, microstructure, and microhardness. Moreover, setting improper welding parameters will contribute to weld defects issue such as expulsion at tested specimens. Welding of titanium alloy and stainless steel become more challenge because these materials are totally different in chemical and thermal properties. As the impact, hard and brittle intermetallic phases occurred. By using aluminium alloy as interlayer, the resistance spot welding between titanium alloy and stainless steel can be achieved. The aim of this project is to investigate the relationship of welding parameters which are weld current and weld pressure towards the mechanical properties of titanium alloy (Ti-6Al-4V) and stainless steel (ASS316L) with aluminium alloy. The research methodology had been identified. The welded specimens are proceeded to tensile strength test to determine the ultimate tensile strength welded joint. Then, microstructure analysis and microhardness test are conducted to examine the effect of welding parameters at welded zone. The result shown the maximum tensile strength is 4.743kN with combination of weld current 11kA, weld pressure 0.35MPa, and weld time 10 cycles. The microstructure of welded specimens observed and further analysed under optical microscope after etching. Besides that, microhardness test conducted is to determine and compare the hardness distribution profile of specimen with highest and lowest tensile strength. As summarised, optimum condition in weld current and weld pressure is one of the crucial factors to achieve better results in tensile strength test, microstructure analysis, and microhardness test.

ACKNOWLEDGEMENT

I would like to express my deep appreciation to my FYP supervisor, Dr Turnad Lenggo Ginta, who gave me advice and guidance in completing this project. His contributions and support helped much in improving my project and make my final year easier. Without your suggestions and guidance, my FYP would not be completed on time.

Then, my sincere appreciation goes to Dr Turnad's master students, Iqbal Taufiqurrahman and Ichwan Fatmahardi, who give me guidance and advice throughout the project especially the usage of resistance spot welding machine and details procedure to conduct the experiment. We cooperate with each other and do a lot of hand on work together during sample preparation and fabrication. I really appreciate the effort they contribute on me. Without them, the project would not be smooth in progress and full of support.

Moreover, I would like to appreciate to all lab technicians especially Mr Johan and Mr Daniel who had assisted me in conducting the experiment for this FYP. Thanks for teaching me how to use the testing equipment and always keep in touch with me regarding the lab slot booking. Without your kindly help, my experiment would not be completed on time.

In the nutshell, I would like to express my thankful to my family who always supporting me and put a lot of concern along my university life. Your supports made my personal life full of caring in final year semesters. Moreover, I would also want to thank my friends who always assist me throughout the final semester. Your helps and supports make my final year wonderful and meaningful.

TABLE OF CONTENTS

CERTIFICATION	ii
ABSTRACT	iv
ACKNOWLEDGEMENT	v
TABLE OF CONTENTS	vi
LIST OF FIGURES	viii
LIST OF TABLES	x
ABBREVIATIONS AND NOMENCLATURES	xi
CHAPTER 1 INTRODUCTION	1
1.1 Background of Study	1
1.2 Problem Statement	3
1.3 Objectives.....	4
1.4 Scopes of Study.....	4
CHAPTER 2: LITERATURE REVIEW	5
2.1 Operation Principle of Resistance Spot Welding.....	5
2.2 Resistance Spot Welding Parameters.....	7
2.2.1 Weld Current.....	7
2.2.2 Weld Pressure (Electrode Force)	8
2.2.3 Weld Time.....	8
2.2.4 Squeeze Time	8
2.2.5 Hold Time	9
2.3 Literature Background of Materials	9
2.3.1 Titanium Alloy (Ti-6Al-4V)	9
2.3.2 Austenitic Stainless Steel 316L(ASS 316L)	10
2.3.3 Aluminium Ally (AA 5754)	10
2.4 Mechanical Properties	10
2.4.1 Tensile Strength	10
2.4.2 Microstructure	12
2.4.3 Microhardness	13

CHAPTER 3: METHODOLOGY	15
3.1 Methods & Tools	16
3.1.1 Specimens Preparation	16
3.1.2 Resistance Spot Welding Experiment	16
3.1.3 Tensile Strength Experiment	18
3.1.4 Microstructure Experiment	19
3.1.5 Microhardness Experiment	23
3.2 Gantt Chart & Project Milestone	24
3.2.1 Gantt Chart	24
3.2.2 Project Milestone	25
CHAPTER 4: RESULTS & DISCUSSIONS	26
4.1 Tensile Strength Test	26
4.2 Microstructure Analysis	31
4.3 Microhardness Test	35
CHAPTER 5: CONCLUSION & RECOMMENDATIONS	39
5.1 Conclusion	39
5.2 Recommendations	40
REFERENCES	41

LIST OF FIGURES

Figure 2.1: Resistance Spot Welding	5
Figure 2.2: Heat Generated in Welding	6
Figure 2.3: Principle Stage (Operating Sequences) in Resistance Spot Welding	6
Figure 2.4: Current-Force Diagram of RSW Machine.....	7
Figure 2.5: Load vs Displacement Curve.....	11
Figure 2.6: Measurement of Weld Nugget.....	12
Figure 2.7: Microstructure at Interfacial Zone: (a) Ti/A5052 (b) A5052/SUS304 ...	13
Figure 2.8: Vickers Hardness Testing Principle	14
Figure 3.1: Process Flow of Project	15
Figure 3.2: Arrangement and Dimension of Specimen.....	17
Figure 3.3: Daiden Spot Welding Machine.....	18
Figure 3.4: Universal Tensile Machine (UTM)	19
Figure 3.5: Auto Mounting Machine	21
Figure 3.6: Grinding Machine.....	21
Figure 3.7: Microhardness Testing Machine	23
Figure 4.1: Specimen in Lap Joint Arrangement	26
Figure 4.2: Fracture Surface from SWS-1 to SWS-6.....	27
Figure 4.3: Image of Specimen with Highest and Lowest Tensile Strength.....	27
Figure 4.4: Plot of Tensile Strength with Weld Current	28
Figure 4.5: Plot of Tensile Strength with Weld Pressure.....	29
Figure 4.6: Cross Section of Welded Joint	31
Figure 4.7: Microstructure for SWS-1	31
Figure 4.8: Microstructure for SWS-2	32

Figure 4.9: Microstructure for SWS-3 32

Figure 4.10: Microstructure for SWS-4 32

Figure 4.11: Microstructure for SWS-5 33

Figure 4.12: Microstructure for SWS-6 33

Figure 4.13: Hardness Distribution on Weld Geometry 35

Figure 4.14: Structure of Weld Region 35

Figure 4.15: Microhardness Distribution Profile for SWS-3 36

Figure 4.16: Microhardness Distribution Profile for SWS-4 38

LIST OF TABLES

Table 2.1: The Chemical Composition of Ti-6Al-4V	9
Table 2.2: The Chemical Composition of ASS 316L	10
Table 2.3: The Chemical Composition of AA 5754	10
Table 3.1: Welding Parameters in Constant Value	17
Table 3.2: Tested Welding Parameters	17
Table 4.1: Experimental data for Tensile Test	27
Table 4.2: Microhardness Results for SWS-3.....	36
Table 4.3: Microhardness Results for SWS-4.....	37

ABBREVIATIONS AND NOMENCLATURES

BM	- Base Metal
HAZ	- Heat Affected Zone
IMC	- Intermediate Layer Compound
RSW	- Resistance Spot Welding
SWS	- Spot Welding Sample
TL	- Transition Layer

CHAPTER 1

INTRODUCTION

1.1 BACKGROUND OF STUDY

Resistance spot welding (RSW) is one primary welding processes wisely apply in aerospace, chemical plant, automotive, and other major industries. This process is important used for sheet metal assembles fabrication. RSW still crucial in industries nowadays mainly is due to its high productivity, high automation, and low manufacturing cost (Wang & Tao & Yang, 2019). During resistance spot welding working process, two or more separated metal sheets are positioned between water-cooled copper alloy electrodes, then heat is obtained by passing large electrical current for welding in a short time period (Kahraman, 2007). This fabrication process needs the interconnection from electrical, thermal, mechanical, and metallurgical phenomena to complete one welding cycle (Mishra, 2016).

Dissimilar metal welds are common in construction of welding and they contribute essential function and excellent performance to construct system structure. Dissimilar metal welding is involved joining of two or more different metal sheets. Thus, joining between titanium alloy and stainless steel with aluminium alloy as interlayer not only saves material, but also gives excellent corrosion resistance and acquires high strength to weight ratio (Hua & Qiu & Cui & Shen & Li, 2015). In this study, the effect of welding parameters is analysed deeply between 3 mm of titanium alloy (Ti-6Al-4V) and austenitic stainless steel 316L (ASS 316L) respectively with interlayer of 2 mm aluminium alloy.

Weld time, electrode force, and weld time are the most important parameters during welding (Ertek Emre & Kacar, 2016). Throughout this study, the investigated welding parameters are weld current and weld force (pressure) while weld time kept

constant. This is because weld current and weld force are the parameters that give higher percentage of contribution compared to weld time by using a statistical analysis technique called analysis of variance (ANOVA) (Mansor & Yusof & Ariga & Miyashita, 2018). Then, AC resistance welding machine with power capacity of 35 kVA and frequency of 50 Hz is used throughout this project. Controlling welding parameters properly are one of the initiatives in this project. The main reason is because small deflection in one of the welding parameters will give direct impact to all other parameters (Raut & Achwal, 2014).

Setting of weld current is crucial in determining the tensile strength, microhardness, and microstructure of welded joint. This is because weld current affect directly the forming of weld nugget because the power supply is directly proportional to square of welding current expressed as, $Q=I^2RT$. Increasing in weld current caused the weld nugget diameter increased as the heat input to the metal sheets increased (Hou & Qiub & Cui & Shen & Li, 2015). Then, weld nugget (fusion zone) also contributes the highest hardness values for welded joints followed by HAZ (Heat Affected Zone) and weld metal in different welding parameters (Kahraman, 2007). Thus, heat generated at metal sheets make the middle of weld nugget reaches maximum hardness. Moreover, original grains growth larger due to thermal gradient of welding process.

Then, adjustment from weld pressure also prominent in deciding the outcome for mechanical properties and microstructure of welded joint. Increasing in weld pressure, enhance the weld strength as joining at high welding parameters is very good (Kahraman, 2007). Also, huge deformation amount at high weld pressure during hold time increase the hardness measurement (Shamsul & Hisyam, 2007). Then, at high pressure, the grains elongated parallel to electrode compression direction and more evident for joined sheet, however for lower pressure, the microstructure (twinning) is not obvious after welding (Kahraman, 2007).

Suitable meshing of welding parameters will contribute an optimum weld quality and good joining at faying area. After welding, welded metal sheets will further investigate in terms of tensile strength, microhardness, and microstructure for different parameters conditions.

1.2 PROBLEM STATEMENT

Proper setting of welding parameters especially weld current, weld force, and weld time are the main challenges in this study. This is because welding input parameters will affect the quality of weld joint in specimens and thus affect the results of experiments in term of tensile test, microhardness test, and microstructure observations. To attain optimum or suitable welding parameters between 3 mm of titanium alloy (Ti-6Al-4V) and austenitic stainless steel 316 L (ASS 316L) with 2 mm of aluminium alloy, it required a time-consuming trial from student in lab, review from others' research, and perspectives of supervisor.

No suitable setting of welding parameters would contribute to occurrence of welding defects which are expulsion, excessive indentation, and cracks. Severe expulsion and deep indentation happened on weld surface due to high weld current will cause decreasing in tensile strength of specimens (Zhang & Zhang & Chen & Yang & He, 2017). If the heat input is not sufficient in faying region, it always will cause initiation of crack under load conditions.

Titanium alloy and stainless steel are difficult to weld because of the variety in physical, chemical, and thermal properties (Hua & Qiu & Cui & Shen & Li, 2015). During welding phase, 3 mm of titanium alloy and stainless steel is difficult to weld due to dissimilar material composition, the joint can be obtained but the weld joint is not strong enough even it broke easily when pulling on welded specimen. The reason is because dissimilar welding might contribute to formation of hard and brittle intermetallic phases (Fe-Ti) which can cause cracking and then reducing the joint strength of specimens (Yu, 2018). Thus, to solve this problem, the selection of intermediate interlayer was used by adding aluminium alloy with 2 mm thickness between titanium alloy and stainless steel to limit the formation of brittle intermediate compound (IMC).

1.3 OBJECTIVES

The aim of this study is to analyse the effect of welding parameters on stainless steel and titanium alloy in thickness of 3 mm with a layer of aluminium alloy in 2 mm. Thus, the detailed objectives of this study are as follow:

- To investigate the effect of welding parameters such as weld current and weld force (pressure) to the mechanical properties of materials in terms of tensile strength, microhardness, and microstructure.
- To study the optimum parameters for weldment between titanium alloy and stainless steel with aluminium alloy as interlayer.

1.4 SCOPES OF STUDY

The scope of study is to ensure the selected welding parameters are suitable for 3 mm thickness of titanium alloy and stainless steel with 2 mm aluminium interlayer. The setting of welding parameters must in the range of favourable condition. The scope of this project is to analyse and evaluate weld pressure (electrode force), weld time, and weld current as small change in setup of welding parameters may give a huge impact towards the weldment of specimens. After spot welding, the specimen samples will be further analysed in mechanical performance in aspects of tensile strength, microhardness, and microstructure.

CHAPTER 2

LITERATURE REVIEW

2.1 OPERATON PRINCIPLE OF RESISTANCE SPOT WELDING

Resistance spot welding (RSW) is a thermo-electric process in which a pair of copper alloy electrodes concentrate heat generated by electric current into metal pieces and clamping the metal pieces simultaneously (Rawal & Inamdar, 2014). The heat energy from electrical current make temperature of metal sheets increased and cause melting at interface of metal sheets, then liquid metal (liquid nugget) appeared. Due to joule heating and contact resistance, a coalescence of metal (also known as weld nugget) is formed at overlapping area of work pieces. When there is an increasing of energy amount into a welding system, more metal will melt to form liquid nugget at overlapping contact (Zhou & Yao, 2019). After liquid nugget reached desired temperature of welding, the weld current delivery terminates, then the liquid nugget solidified and the separated metal sheets joined together (Zhou & Yao, 2019). During welding, the maximum weld current is depended on load resistance and capacity of electrical system.

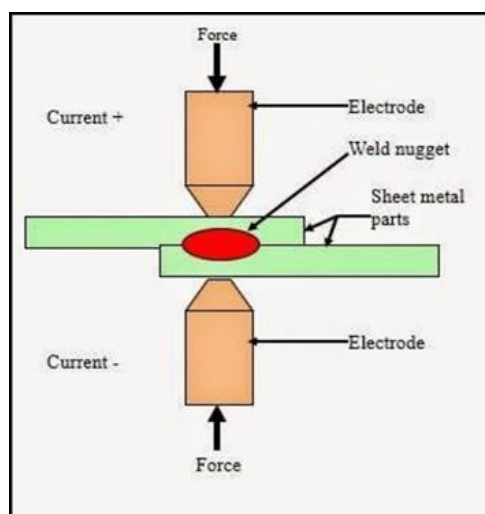


Figure 2.1: Resistance Spot Welding Process

Then, the RSW process is depended on 4 factors, which are the amount of weld current, pressure applied from electrodes, time current flow, and area of electrode tip contact on metal piece (Faiyaz & Borke, 2017). Thus, to produce good quality of weld, welding parameters must be controlled properly.

Due to the resistance of base metal to electrical current flow, the heat generated is limited to the contact of weld area and tips of electrode (Faiyaz & Borke, 2017). When welding force (or weld pressure) is applied, the heat is generated. Basically, the heat generated in welding process is depend on electrical current and time used on electrical resistance between electrodes and materials. The basic formula for heat generated in resistance spot welding process according to Joule's Law is stated as (Rawal & Inamdar, 2014):

$Q = I^2 R t$	<p>Q: heat generated (J), I: welding current (A), R: resistance of the work piece(Ω), t: time of current flow (sec).</p>
---------------	---

Figure 2.2: Heat Generated in Welding

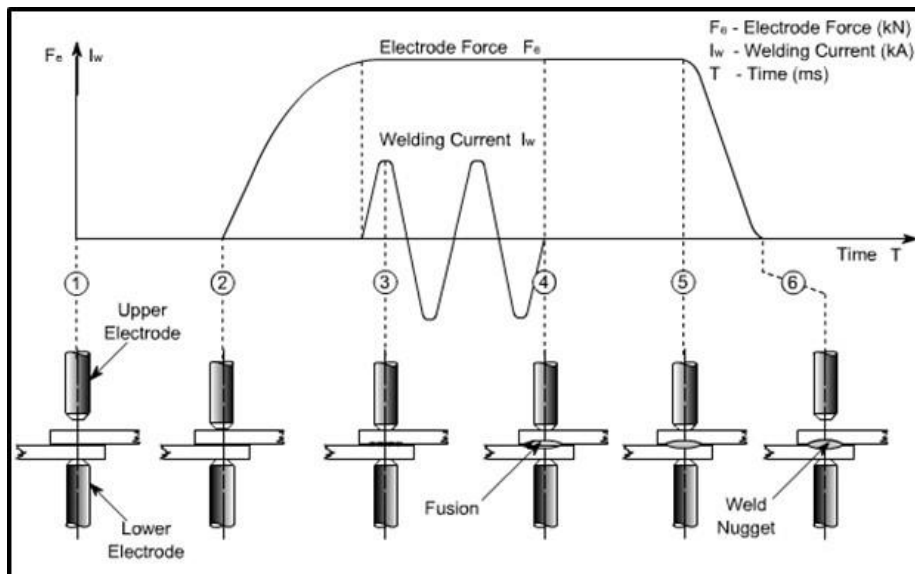


Figure 2.3: Principle Stages (Operating Sequences) in Resistance Spot Welding

In cycle of resistance spot welding, there are many stages in a short period of time (Shelly & Sahota, 2017). The first step is squeezing, the upper electrode clamp toward lower electrode. Then, force from pneumatic cylinder will make 2 metal workpieces contact well in order to supply proper contact resistance for heat generation. The next step will be welding as weld current is conveyed by electrode to workpieces

(Shelly & Sahota, 2017). At this stage, the energy generated from current melts the contact area of workpiece. The third step of RSW is cooling. Cooling phase (hold time) is important for liquid nugget to cool down, so it will become strong and solid weld nugget. On this step, electrode remains on the workpieces to hold the joints together. The final step is moving away workpieces by lifting the electrodes by leg pedal, then production of one spot weld ends.

2.2 RESISTANCE SPOT WELDING PARAMETERS

The major welding parameters in spot welding are weld current, weld force, and weld time. Other than these, other parameters such as squeeze time and hold time that can be controlled in welding machine also crucial in spot welding. Hence, control properly above welding parameters must be practised well to produce good quality of weld (Gawai & Sedani, 2016).

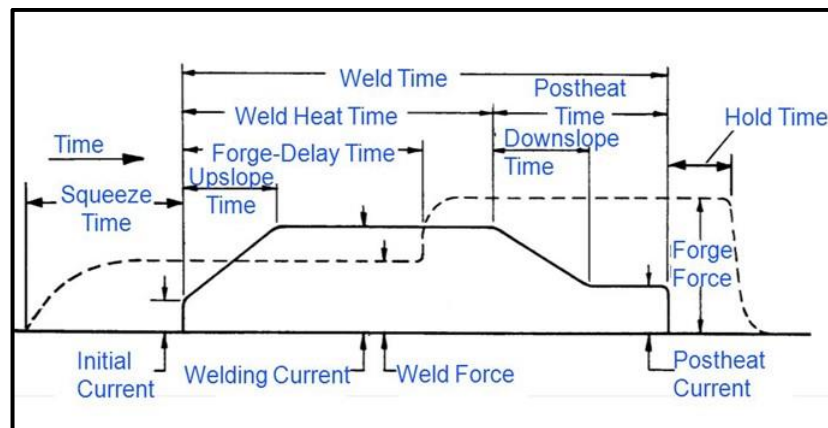


Figure 2.4: Current-Force Diagram of RSW Machine

2.2.1 Weld Current

Weld current is the heat required in welding circuit to make a weld. Heat generated in resistance spot welding is directly proportional to weld current (Nasir & Khan, 2016). Thus, the weld current recommended to be kept as low as possible (Asari, 2018). However, too low weld current will cause insufficient heat supply to weld nugget formed. Then, increasing in current density of course will increase tensile shear strength as increasing in weld nugget diameter. However, excessive current will

overheat the metal and cause the weld in low mechanical strength properties, weld cracking, molten weld expulsion, and high potential of deep indentation at metal sheets surface (Gawai & Sedani, 2016).

Commonly the weld current amplitude is at the range of 5kA to 10kA based on weld requirement, sheet configuration, and other process parameters (Nasir & Khan, 2016). So, weld current level is important in deciding the size of heat affected zone (HAZ) and distortion of weld metal.

2.2.2 Weld Pressure (Electrode Force)

Electrode force applied purposely is to keep and press metal sheets to be joined together in contact at joint interface. Large electrode force is required to ensure the weld quality is good enough. However, too large electrode force will distribute to occurrence of other side effects. Increasing in electrode force will cut down the heat energy in welding, so higher value of electrode force must need higher setting of current (Asari, 2018). Controlling electrode force is crucial in welding as repeatable weld force can provide consistent welds.

2.2.3 Weld Time

Weld time is the time duration for weld current applied to metal sheets. In AC system, the weld time is expressed and adjusted in cycle (Nasir & Khan, 2016). Normally, one cycle is equal to 1/50 second in a 50 Hz of power system (Asari, 2018). Then, the heat generated is proportional to weld time and minimum weld time is to ensure good weld quality. The weld time set is depending on thickness, coating, and properties of material.

2.2.4 Squeeze Time

Squeeze time is the amount of time that electrode force is applied before the flow of weld current. Squeeze time is important to delay weld current when electrode has reached the preset force level (Asari, 2018). The purpose of squeeze time is to stabilize the electrode tip before any applied current. If weld current applied under

condition of unstable force at electrode tip, several problems will happen. It included surface and interfacial expulsion, electrode wear, and arcing (or weld splash).

2.2.5 Hold Time

Hold time is the cooling period of welding, when electrodes are still applied to sheet to chill the weld. Hold time is essential in solidification of weld nugget. If the cooling time is too long, the weld will spread heat to electrode and the electrode will has high potential exposed to wear (Asari, 2018).

2.3 LITERATURE BACKGROUND OF MATERIALS

2.3.1 Titanium Alloy (Ti-6Al-4V)

Ti-6Al-4V (ASTM Grade 5) is a metal that mixed with titanium and other chemical elements. It classified as alpha-beta alloy and have 2 phase microstructures formed by up to 6% aluminium and difference amounts of beta components such as vanadium, chromium, and molybdenum. Usage of titanium alloy has brought reliable performance in aerospace, chemical plant, automotive, and other major industries due to its low weight ratio, high strength level, excellent in high temperature properties, and good corrosion resistance (Ahmed & Sahari & Ishak & Khidhir, 2014). The chemical composition of titanium (Ti-6Al-4V) alloy used in this study is shown as Table 2.1 (Zhang & Zhang & Chen & Yang & He, 2017) with the density of 4.43 g/cm³ (Singh & Pungotra & Kalsi, 2017).

Table 2.1: The Chemical Composition of Ti-6Al-4V

Components	Al	V	Fe	Si	O	C	N
wt (%)	6.15	3.96	0.3	0.02	0.2	0.37	0.01

2.3.2 Austenitic Stainless Steel 316L (ASS 316L)

ASS 316L is a type of austenitic stainless steel that consists microstructure of ferrite and austenite (Kianersi & Mostafaei & Amaded, 2014). It widely used in industrial application because of excellent weldability, high corrosion resistance, and decorative appearance. The chemical composition of austenitic stainless steel (ASS 316L) used in this study is shown as Table 2.2 (Bharath & Sridhar, 2014) with the density of 8.03 g/cm³.

Table 2.2: The Chemical Composition of ASS 316L

Components	C	Mn	P	S	Si	Cr	Ni	N	Mo
wt (%)	0.08	2.00	0.045	0.030	0.75	16-18	10-14	0.10	2-3

2.3.3 Aluminium Alloy (AA 5754)

AA 5754 is an aluminium alloy that consists highest composition percentage of aluminium contents. The chemical composition of AA 5754 used as interlayer in this project experiment is shown at Table 2.3 (Casalino & Facchini & Mortello & Mummolo, 2016). It is the common material used in automobile due to excellent weldability, high strength, low density, and can withstand corrosion (Mercan & Ayan & Kahraman, 2019).

Table 2.3: The Chemical Composition of AA 5754

Components	Si	Fe	Cu	Mn	Mg	Cr	Zn	Ti	Al
wt (%)	0.40	0.40	0.10	0.50	2.6-3.6	0.30	0.20	<0.15	balance

2.4 MECHANICAL PROPERTIES

2.4.1 Tensile Strength

Tensile strength is the maximum capacity of a material to withstand load without fracture in tension direction. Generally, tensile test is a common method used to evaluate the behaviour of weldment joint in static condition (Mansor & Yusof & Ariga & Miyashita, 2018). After welding, tensile test is the direct approach to measure the tensile strength. The reason of conducting tensile test is because welding

parameters have obvious influence on the tensile strength of specimens (Zhang & Zhang & Chen & Yang & He, 2017). Figure 2.5 shows the load vs displacement curve and how the ultimate tensile strength (UTS) is measured for weldment of titanium alloy (Ti-6Al-6V), aluminium alloy (AA5754), and stainless steel (ASS316L).

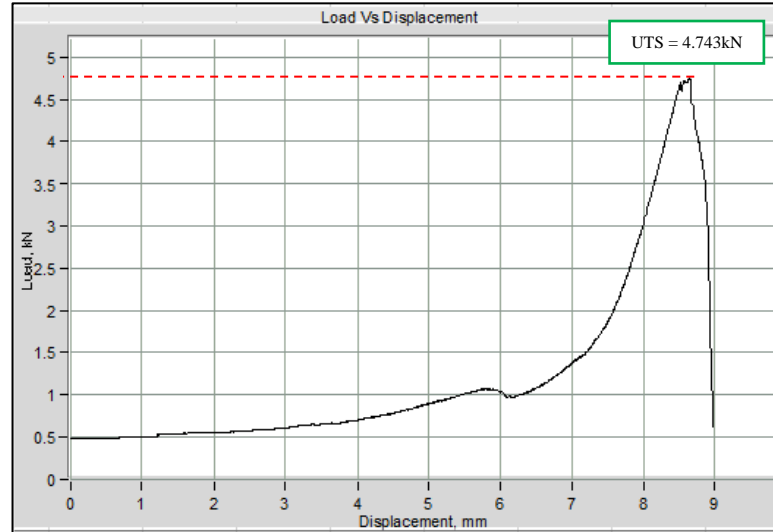


Figure 2.5: Load vs Displacement curve

Increasing in welding parameters are contributed to higher tensile strength because huge weld nugget size covers the weld zone of specimen during welding (Das & Das & Paul, 2020). As the results, shearing resistance on load application is higher, which caused the specimen not easy to fracture in pulling direction. Moreover, the welded specimens are failed in interfacial mode as the cracks propagated through weld nugget during tensile shear test (Das & Das & Paul, 2020).

The tensile strength of welded specimen can be determined directly by using Universal Tensile Machine (UTM). It also can be calculated by using Eq 2.1. This generated equation is essential to analyse ultimate tensile strength of tested specimens theoretically. Moreover, the diameter of weld nugget is computed by using Eq 2.2, which is needed in Eq 2.1.

$$\textit{Tensile Strength} = \frac{\textit{Maximum Load (N)}}{\textit{Area of weld nugget (m}^2\textit{)}} \quad \text{Eq 2.1}$$

where area of weld nugget is $A = \frac{\pi}{4} d^2$

$$\text{Average Diameter} = \frac{D1+D2}{2}$$

Eq 2.2

where D1 is the largest weld diameter in meter, D2 is the smallest weld diameter in meter.

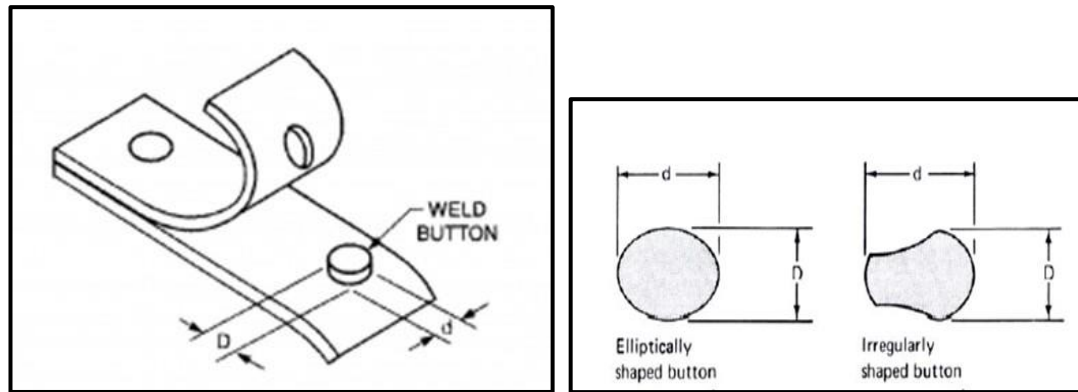


Figure 2.6: Measurement of Weld Nugget

2.4.2 Microstructure

Microstructure can be explained as very small scale structure of a material which need magnification under optical device. From microstructure analysis, weld defects also can be detected to determine whether the setting of welding parameters are in optimised condition for the materials (Zhang & Zhang & Chen & Yang & He, 2017).

From previous study, the purpose of microstructure experiment is to observe the change in microstructure of materials at interfacial zone of titanium alloy/aluminium alloy and stainless steel/aluminium alloy after welding process, as shown in Figure 2.7 (Tu & Qiu & Shi & Zhang & Zhang, 2011). Through the observation from Figure 2.7(a), it shows the diffusion reaction occurs between titanium base metal and aluminium (A5052) while in Figure 2.7(b), it shows the reaction between aluminium (A5052) and stainless steel (SUS304), which is a serrate morphology at A5052 and a flat layer at SUS304 (Tu & Qiu & Shi & Zhang & Zhang, 2011). Thus, the microstructure of dissimilar material such as titanium, aluminium, and stainless steel after resistance spot welding should be closed to the image in Figure 2.7.

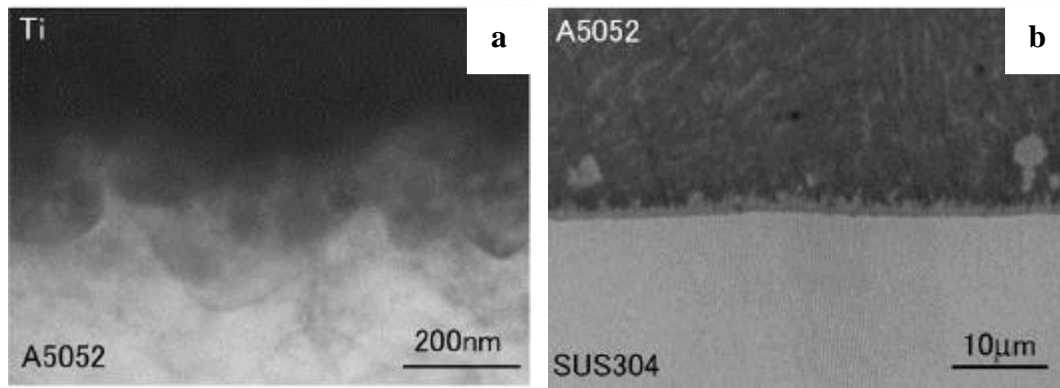


Figure 2.7: Microstructure at Interfacial Zone: (a) Ti/A5052 (b) A5052/SUS304

2.4.3 Microhardness

Microhardness can be explained as resistance of a material to deform plastically by indentation or abrasion. The microhardness test is one of the experiment to determine mechanical properties for a small volume of materials. Usually, the standard procedure for expressing the relationship between indentation size and hardness are Brinell hardness test, Vickers hardness test, and Rockwell hardness test. Every hardness test has different types of indenters. In this study, Vickers hardness test is used because this method is the most sensitive and accurate testing for welded material (Petrik & Palfy, 2011)

Vickers hardness test is an optical measurement system by using a diamond indenter to make an indentation. This indentation is measured, then converted into a hardness value. As the result, smaller the indentation size, harder the material because the particular material is difficult to plastically deformed under the indenter (Petrik & Blasko & Durisin & Vasilnakova & Guzanova, 2019). Then, increasing in microhardness profile indicate the tensile strength of material also increased (Mittal & Gupta & Pratap & Shukla & Gupta & Shanurrahman, 2020).

Thus, the microhardness of specimen can be determined directly using microhardness testing machine by providing the d_1 , d_2 , and load. However, Vickers hardness (HV) value of material also can be measured and checked by using Eq 2.3 (Li & Xue & Zhao & Wang & Wang & Song, 2019).

$$HV = \frac{2F \sin \frac{136^\circ}{2}}{d^2} = 1.854 \frac{F}{d^2} \quad \text{Eq 2.3}$$

where F is load in kgf, d is the average value of d_1 and d_2 in mm.

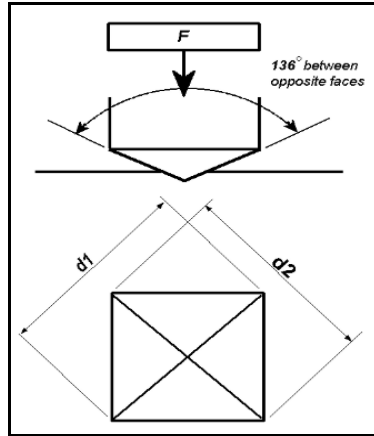


Figure 2.8: Vickers Hardness Testing Principle

CHAPTER 3

METHODOLOGY

Methodology is a research strategy applied in one study field. It composed of knowledge principle and theoretical analysis. In this chapter, comprehensive procedures, tools and equipment used in this study would be discussed clearly. Then, Gantt chart and project milestone in this study also would be presented.

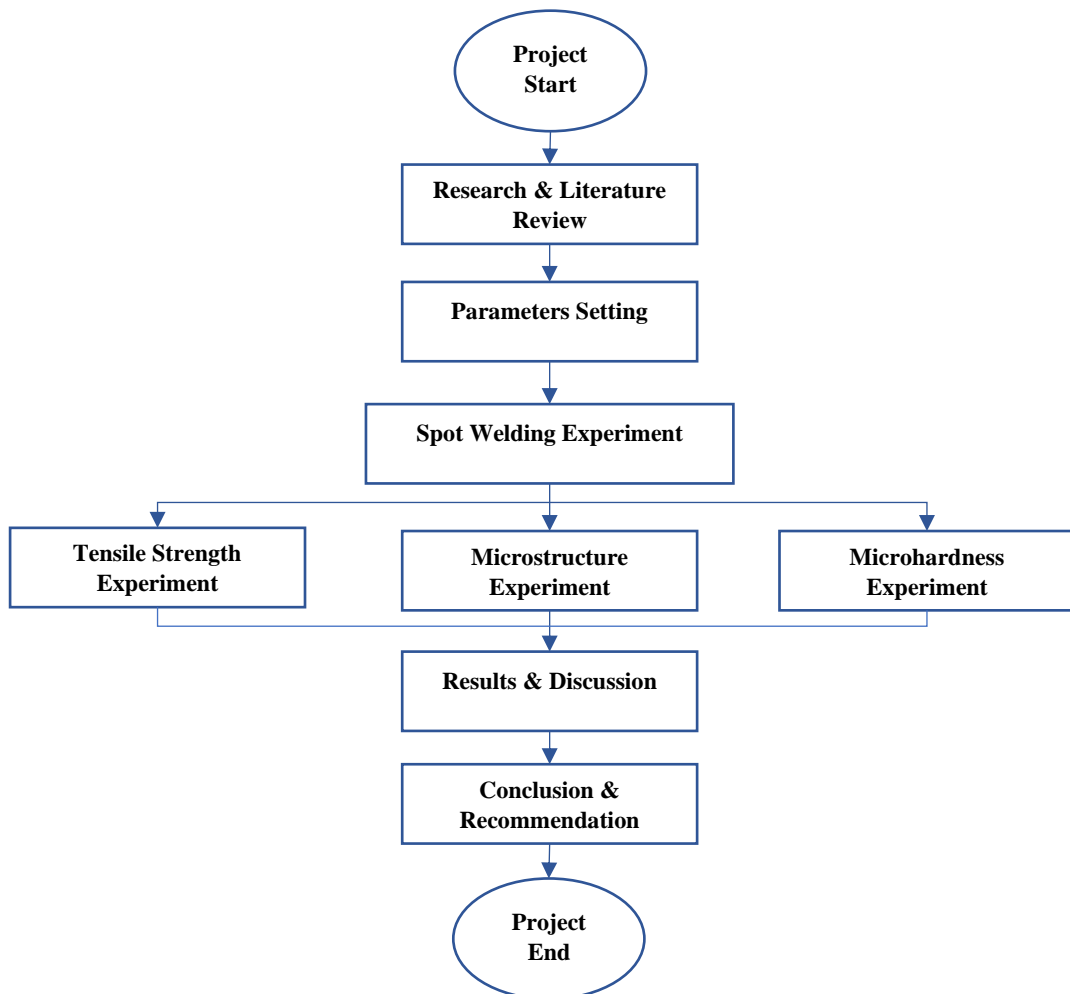


Figure 3.1: Process Flow of Project

3.1 METHODS & TOOLS

3.1.1 Specimens Preparation

Titanium alloy (Ti-6Al-4V) and austenitic stainless steel 316L (ASS 316L) were used for the upper and lower parts of welding specimen. The specimens are in 3 mm thickness respectively. The 2 mm of aluminium alloy placed between 2 metals. All the specimens were cleaned after cutting.

Equipment Used: (i) Laser cut machine
(ii) Wire cut machine
(iii) Digital vernier calliper
(iv) Silicon carbide (SiC) abrasive paper
(v) Ethanol

Procedures:

- i. Ti-6Al-4V is prepared and cut by wire cut machine.
- ii. ASS 316L is prepared and cut by laser cut machine.
- iii. Dimension of specimens by measured by digital vernier calliper to get the desired dimensions (length: 100 mm, width: 25 mm).
- iv. Aluminium alloy is prepared and cut by notching machine. The desired dimension are length and width with 25 mm respectively.
- v. Grinding every cut metal by using abrasive paper to remove cutting burr. Then, clean the surface impurities by ethanol.
- vi. Put the all specimens into labelled container.

3.1.2 Resistance Spot Welding Experiment

The experiment was based on the standard mentioned in chapter 2. Weld current and weld force (pressure) would be tested to obtain the optimum results of welding parameters for Ti-6Al-4V and ASS 316L.

In Table 3.1, it shown the constant welding parameters during welding. According to the standards GB 2651-88 (Tensile test standard on weld joint, China), the arrangement and dimension of specimen for tensile test is mentioned in Figure 3.2.

Then, in Table 3.2, it also shown the tested welding parameters throughout the testing. In Table 3.2, increment of 10% and 20% for weld current and weld force (pressure).

Table 3.1: Welding Parameters in Constant Value

Squeeze Time (cycle)	Up-slope (cycle)	Hold Time (cycle)
45	2	15

Table 3.2: Tested Welding Parameters

Material	Specimen No.	Weld Current (kA)	Weld Pressure (MPa)	Weld Time (cycle)
Ti-6Al-4V & ASS 316L (Al alloy as interlayer)	SWS-1	11.00	0.30	20
	SWS-2	12.10		
	SWS-3	13.30		
	SWS-4	11.00	0.35	20
	SWS-5	12.10		
	SWS-6	13.30		

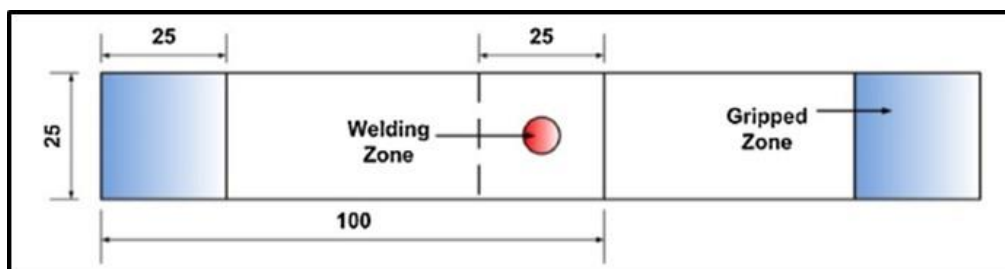
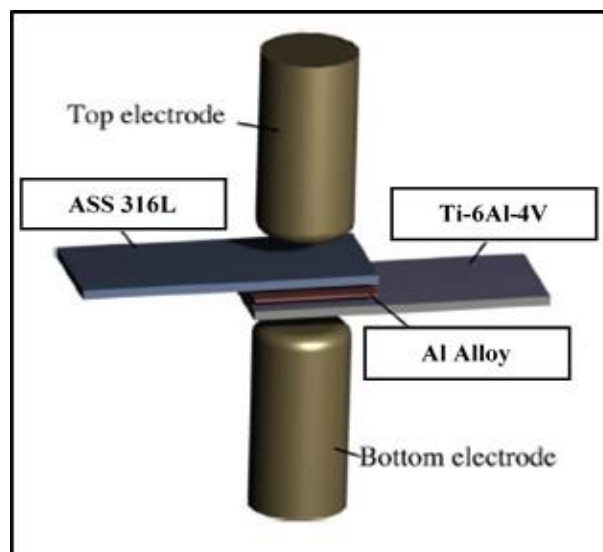


Figure 3.2: Arrangement and Dimension of Specimen

Equipment Used: (i) Safety goggles & gloves

(ii) Daiden spot welding machine (Type: L-AJ 35-600)

Procedures:

- i. Wear the personal protective equipment (PPE) before starting the experiment.
- ii. Set the value of constant welding parameters shown in Table 3.1 at controller.
- iii. Set the weld current of 11 kA, electrode force of 0.35 MPa, and weld time of 20 cycle for SWS-1.
- iv. Press the leg pedal to start welding.
- v. Step (iii) and (iv) was repeated for SWS-2 to SWS-6.



Figure 3.3: Daiden Spot Welding Machine

3.1.3 Tensile Strength Experiment

Tensile test used in this study is to evaluate the quality of welded joint and maximum stress needed for a material to undergo necking. The samples were pull at universal tensile machine (UTM) with load of 50kN and speed of 10 mm/min. Before starting the experiment, all the specimens are strongly clamped at universal tensile machine. Ultimate tensile strength value and graphs are recorded for 6 specimens after the tensile strength experiment.

Equipment Used: (i) Universal tensile machine (UTM)
(iii) Digital vernier calliper

Procedures:

- i. Welded specimens labelled from SWS-1 to SWS-6 are machined in desired orientation according to the standard.
- ii. Load of 50kN and speed of 10 mm/min are set according to type of specimens. Maximum breaking load with graph is recorded after tensile test.
- iii. Measure the diameter of weld nugget by digital vernier calliper.

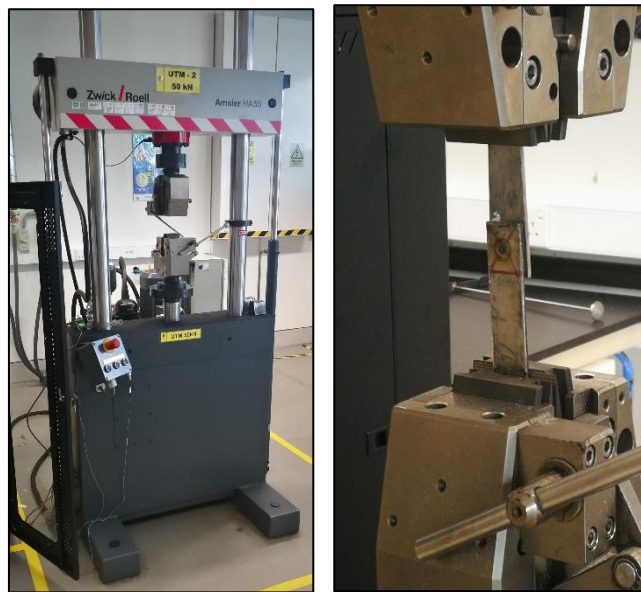


Figure 3.4: Universal Tensile Machine (UTM)

3.1.4 Microstructure Experiment

After welding, there are several processes needed to be done to prepare metallographic specimen. The steps are sectioning, mounting, grinding, polishing, and etching before observing the microstructure under optical microscope.

a) Sectioning

Sectioning is the process of cutting a portion of part from the welded specimens. The part to be sectioning is at the cross section of weld joint. Abrasive cutter is used to cut the welded specimen into desired portion. Then, low cutting speed are required

to get rid of heat damaged to the specimen. Proper cutting procedures must be followed to avoid any accident happen.

Procedures:

- i. Put the desired portion of specimen to be cut at vise on slotted table.
- ii. Place locking lever in forward position which allow control rod moves to the furthest position.
- iii. Tighten the nuts to make sure vise fixed on slotted table.
- iv. Push the control rod to make the specimen contact firmly with cutting wheel.
- v. Turn on the coolant and apply desired pressure until the specimens is sectioned.

b) Mounting

After sectioning, mounting process will be conducted. The purpose of mounting is to make the sectioning part easier to handle during grinding and polishing phase. The sectioning part is mounted in black epoxy thermosetting powder (a mixture of resin and hardener) by using auto mounting press machine. Before mounting, setting of heat time is 1.30 min, cool time is 4.10 min, and pressure is 1300psi.

Procedures:

- i. Raise the ram of machine and locate the cutted specimen.
- ii. Lower slightly the ram with specimen and pour black epoxy thermosetting powder to full cover the specimen.
- iii. Lower the ram again and screw on the bayonet cover.
- iv. Check the setting, which are heating and cooling temperature, heating and cooling time. After that, press the start button.
- v. After the time is finished, lower the ram and remove the bayonet cover.
- vi. Lift the ram and remove the completed mounted specimen.



Figure 3.5: Auto Mounting Machine

c) Grinding

The next process after mounting will be the grinding process. Silicon carbide (SiC) abrasive paper with suitable grit size and grinder are used to grind the surface of mounted specimen. The purpose of grinding is to remove residue layer covered at specimen and to produce a flat surface.

Procedures:

- i. Safety goggles must be worn during the experiment.
- ii. Get a silicon carbide (SiC) paper and place on grinder. Make sure the paper is flat when placing on grinder.
- iii. Switch on the power of grinder and turn on the running water.
- iv. Hold the mounted specimen and grind in one direction under the running water.
- v. Check the surface after every 5 minutes.
- vi. Stop grinding after achieving sufficient smoothness on the surface.



Figure 3.6: Grinding Machine

d) Polishing

The specimen is performed polishing after the grinding process. The specimen is polished with a polishing cloth, lubricant, and diamond polishing compound (3 & 6 micron) to produce a free scratch finishing surface. Generally, the polishing process always done by using diamond abrasive due to smaller multiple cutting edges which can reduce the surface damage of specimen.

Procedures:

- i. Make sure the specimen is cleaned after grinding.
- ii. Stick the polishing cloth onto the platen.
- iii. Spray the lubricant and diamond polishing compound onto the cloth. This process does not involve water.
- iv. Polish the specimen with small amount of force and the time taken should less than 5 minutes.

e) Etching

The purpose of etching is to optically increase the microstructure features of specimen in terms of phase structure and grain size. The specimen is etched under Kellers Etch (Ti-6Al-4V & Al) and Carpenters Etch (ASS316L).

Procedures:

- i. Gloves is compulsory during etching process.
- ii. Placed the specimen on the table of fume hood and tuned on the fume hood.
- iii. Cleaned the surface of specimen by ethanol. Touching is not allowed at treated surface.
- iv. First, etched Ti-6Al-4V and aluminium alloy with Kellers Etch.
- v. After few second, rinse the specimen with water. Then, quickly rinse again the specimen with ethanol.
- vi. After observing the microstructure of Ti-6Al-4V/Al interface, etched ASS316L with Carpenters Etch. Step (v) is repeated before optical microscope.

3.1.5 Microhardness Experiment

Microhardness test is one of method to examine the property of material to resist permanent deformation by penetration. In this experiment, Vickers hardness test will be conducted on the specimens. The reasons are because the indenter size of Vickers test is much smaller which can reduce damage to tested specimens. Besides, it has wide scale of measurement compared to other microhardness test.

In Vickers hardness test, it consists of a diamond indenter with the shape combined of right pyramid and square base. The angle of 136° is subjected to force of 200gf and dwell time of 15 seconds. After indentation, 2 diagonals will display on the surface of specimens and average Vickers hardness calculate under the microscope. The calculation is based on the sloping surface area of indentation.

Equipment Used: (i) Microhardness Testing Machine

Procedures:

- i Placed the mounted specimen on vice of microhardness testing machine.
- ii Lower the indenter until contact the surface of mounted specimen.
- iii Set the desired load and time for indenter.
- iv Raised the indenter from specimen after penetration.
- v The Vickers hardness (HV) is display after key in the D1 and D2.
- vi Repeated steps from (i) to (v) for 5 times at various location of specimen to measure the average HV.



Figure 3.7: Microhardness Testing Machine

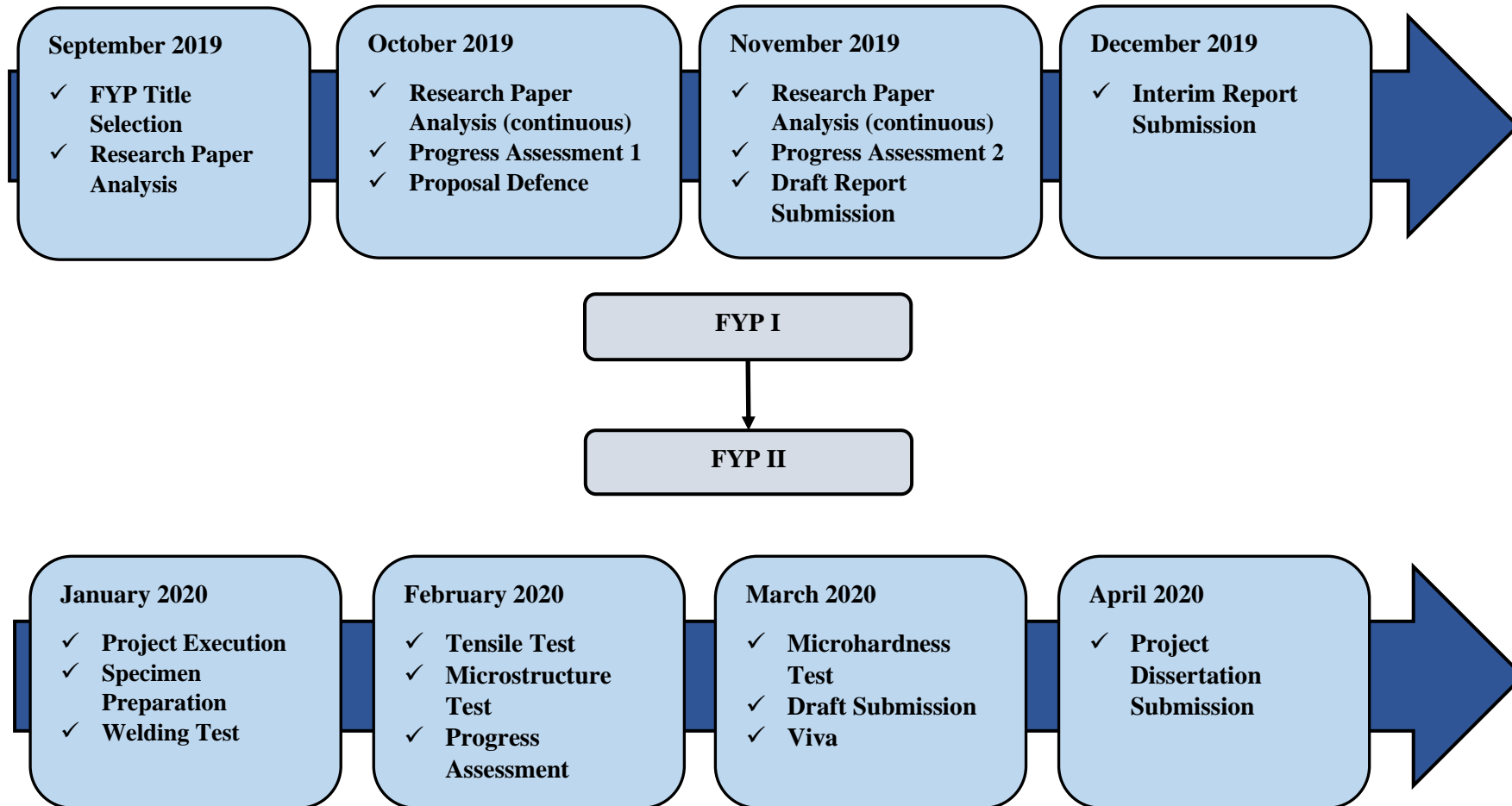
3.2 GANTT CHART & PROJECT MILESTONE

3.2.1 Gantt Chart

Project Flow (FYP I)	Weeks													
	1	2	3	4	5	6	7	8	9	10	11	12	13	14
Project Title Selection	■													
Analysing Related Research Paper		■	■	■	■	■	■	■	■	■	■	■	■	
Progress Assessment						■					■			
Proposal Defence								■	■					
Draft Report Submission												■	■	
Interim Report Submission														■

Project Flow (FYP II)	Weeks													
	1	2	3	4	5	6	7	8	9	10	11	12	13	14
Specimens Preparation	■	■	■											
Resistance Spot Welding Experiment	■	■	■											
Tensile Strength Experiment				■	■									
Microstructure Experiment					■	■	■							
Microhardness Experiment							■	■	■					
Data Analysis and Verification									■	■	■	■		
Progress Assessment						■						■		
Draft Dissertation Submission									■	■				
Viva												■		
Project Dissertation Submission														■

3.2.2 Project Milestone



CHAPTER 4

RESULTS & DISCUSSIONS

4.1 TENSILE STRENGTH TEST

Tensile strength test is the most general method applied to evaluate the mechanical properties of resistance spot welding joint. From the tensile strength test, maximum load can be obtained from load displacement curve to describe the mechanical behaviours of welded joint. The Figure 4.1 shown the welded specimen before tensile strength test.



Figure 4.1: Specimen in Lap Joint Arrangement

In this section, the tensile strength of specimens with different combination of weld current and weld pressure were determined by tensile test. The tensile test was conducted with load of 50kN and pulling rate of 10mm/min. A total of 6 combinations of input parameters were tested. In Table 4.1, it shown the experimental results of tensile testing together with the measurement of each weld diameter. Then, the effect of welding parameters on tensile strength are summarized as plot in Figure 4.4 and Figure 4.5.

Table 4.1: Experimental data of Tensile Test

Sample	Weld Current (kA)	Weld Pressure (MPa)	Weld Time (cycle)	Tensile Strength (kN)	Average Weld Diameter (mm)
SWS-1	11.00	0.30	20	2.982	9.25
SWS-2	12.10	0.30	20	3.192	9.50
SWS-3	13.30	0.30	20	1.369	5.10
SWS-4	11.00	0.35	20	4.743	11.50
SWS-5	12.10	0.35	20	3.306	9.75
SWS-6	13.30	0.35	20	1.748	5.60



Figure 4.2: Fracture Surface from SWS-1 to SWS-6

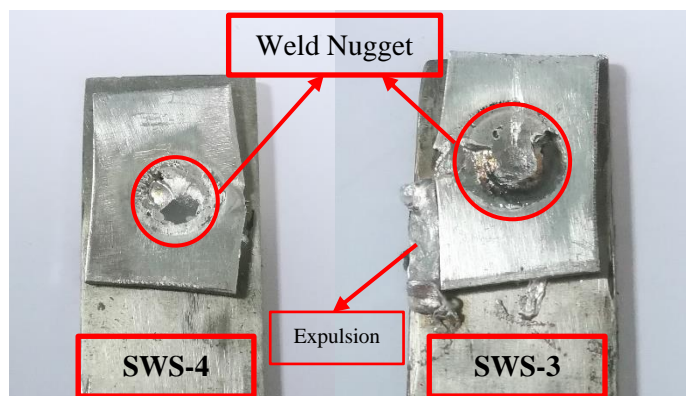


Figure 4.3: Image of Specimen with Highest and Lowest Tensile Strength

According to Figure 4.2, the fracture behaviour of specimens after tensile test is in brittle failure. However, the weldment condition is much better than without aluminium as interlayer. Through Figure 4.3, it shown the characteristic of weld formation after fracture. A perfect weld is formed at SWS-4 as it free of defect rate especially expulsion and undersized weld. In contrast, expulsion occurred at SWS-3

which forming the empty void at aluminium surface. This weld imperfection will reduce the joint strength as less contact area between Ti-6Al-4V and aluminium alloy. Thus, the specimen 3 is more brittle compared to specimen 4 during tensile test.

Based on Table 4.1, the optimum welding parameters condition through this tensile strength experiment is SWS-4 with weld current of 11kA, weld pressure of 0.35MPa, and weld time of 20 cycle. This is because the specimen achieved the highest tensile strength (4.743kN) and average weld diameter (11.50mm). Then, according to Table 4.1, the results of tensile strength merged with weld diameter. As the weld diameter increases, the tensile strength supposed to be increased (Mansor & Yusof & Ariga & Miyashita, 2018). When the size of weld nugget is bigger, larger pulling force is needed to cause the specimen to fracture.

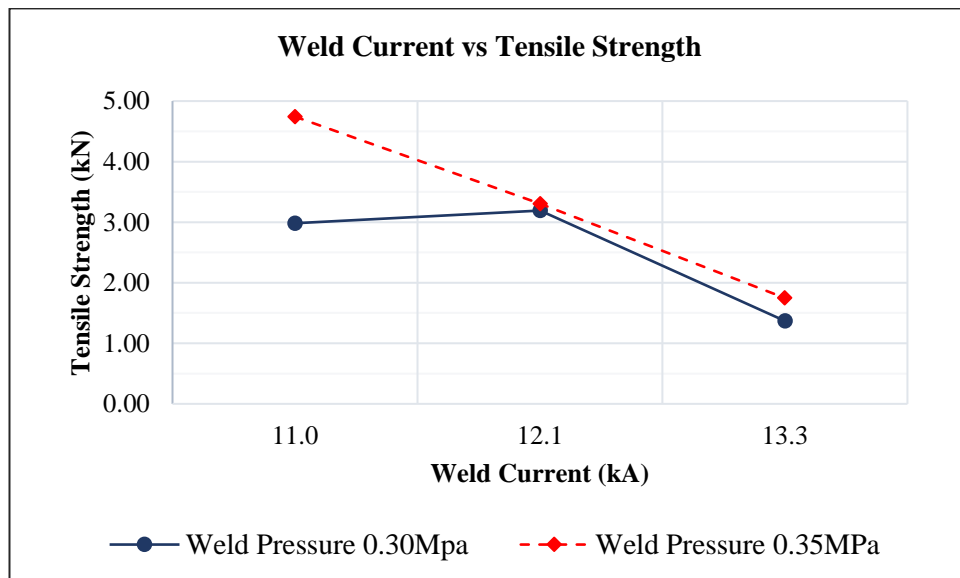


Figure 4.4: Plot of Tensile Strength with Weld Current

The weld current is significant towards the tensile strength of specimens during tensile test. Through the plot from weld pressure 0.30MPa in Figure 4.4, it shown that increasing in weld current from 11.0 to 12.1kA will increase slightly the tensile strength of specimen from 2.982 to 3.192kN. This is because increasing in weld current will rise the growth of weld nugget. This cause the tensile strength to be increased as the weld joint is depended on weld nugget size. However, the tensile strength dropped extremely from 3.192 to 1.369MPa when the weld current increase from 12.1kA to 13.3kA. This could be caused by expulsion during welding due to too high of weld current with low weld pressure setting (Mansor & Yusof & Ariga & Miyashita, 2018).

Thus, excessive heat generated between base metal of Ti-6Al-4V and ASS 316L will make the aluminium alloy at interlayer become thinner, which can limit the growth of weld nugget size. As consequences, the tensile strength decreased as the weld joint is weak at 13.3kA due to expulsion.

On the other hand, when weld current increased from 11.0 to 13.3kA, the tensile strength decreased from 4.743 to 1.748kN at weld pressure of 0.35MPa in Figure 4.4. However, this plot maybe has same trend as the previous plot (weld pressure 0.30MPa), which at first the weld current of 11kA give the tensile strength up to 4.743kN, then tensile strength decreased drastically when current increased from 12.1kA to 13.3kA. The weld current of 11kA at 0.35MPa hits the maximum tensile strength because the welding parameters (weld current & weld pressure) are in the optimum condition. Then, when weld current increased from 12.1 to 13.3kA, the tensile strength decreased intensely from 3.306 to 1.748MPa. For the reasons, higher the weld current, higher the chance specimens contributed to brittle weld (Mansor & Yusof & Ariga & Miyashita, 2018). Thus, at weld current of 13.3kA, the tensile strength is much lower compared to 12.1kA.

From Figure 4.4, both plots can be analysed as the tensile strength will increase to maximum when optimum weld current is achieved. However, further increasing in weld current might decrease the tensile strength of specimens due to brittle weld caused by expulsion.

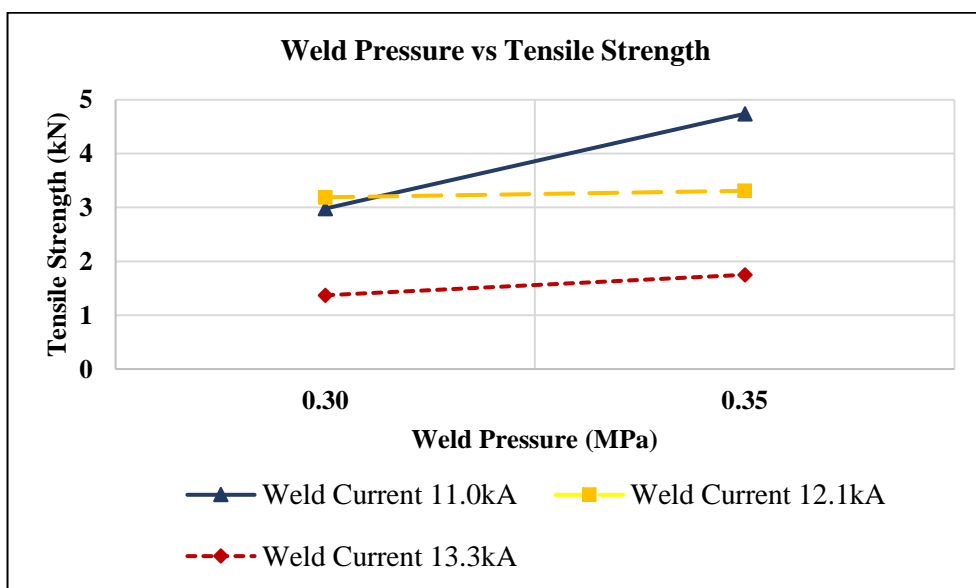


Figure 4.5: Plot of Tensile Strength with Weld Pressure

The effect of weld pressure also important in analysing the tensile strength of specimens. Through Figure 4.5, the tensile strength increased as the weld pressure increased from 0.30 to 0.35MPa. There are many reasons why tensile strength increased when weld pressure increased. Firstly, 0.35MPa probably is the optimum weld pressure for 11.0, 12.1, 13.3kA when compared to weld pressure of 0.30MPa. Lower weld pressure will produce more heat thus expulsion occurs (Mansor & Yusof & Ariga & Miyashita, 2018). Secondly, increasing of 0.05MPa in weld pressure maybe reduce the excessive heat generated during welding, hence the defects rate can be reduced. Thus, tensile strength increased as the weld nugget size grow up without expulsion and porosity.

From the overall observation obtained, increase in weld current will decrease the tensile strength. This is because excess weld current will lead to occurrence of defect rate at welded joint. However, increase in weld pressure increase the tensile strength. This is because the weld pressure of 0.30MPa is too low and not sufficient enough to balance with the weld current set compared to 0.35MPa. Thus, there is a slight increase in tensile strength due to optimization of weld pressure with weld current. When the tensile strength of specimen is lower enough, a weak welded joint is formed. A weak welded joint always can be related with brittle weld. Brittle weld can be defined as weld zone undergoes little plastic deformation before fracture. Thus, phenomenon of decreasing in tensile strength occurs.

4.2 MICROSTRUCTURE ANALYSIS

Microstructure analysis is a method to observe the specimen with magnified image under optical microscope. The microstructure determines the physical and mechanical properties of welded joint. Figure 4.6 shows the cross section of welded joint which fabricated by resistance spot welding. From the picture, a drum shape weld nugget formed at aluminium alloy due to clamping force of electrodes in resistance spot welding. Obviously, there is not fusion zone at interface of base metal because the coalescence process is involved dissimilar material.



Figure 4.6: Cross Section of Welded Joint

After etching with chemical solution, sample 1 to sample 6 are being observed under optical microscope and the microstructure of every sample will be further analysed. Figure 4.7 to Figure 4.12 shows the microstructure image of welded joint with suitable magnification.

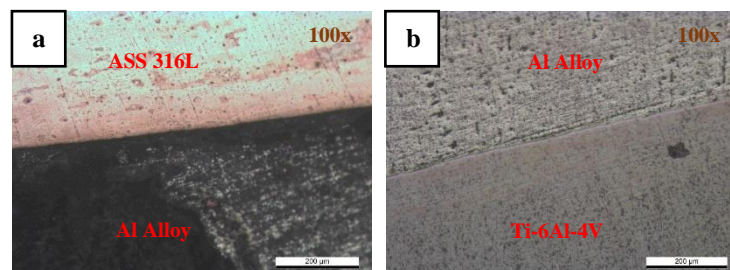
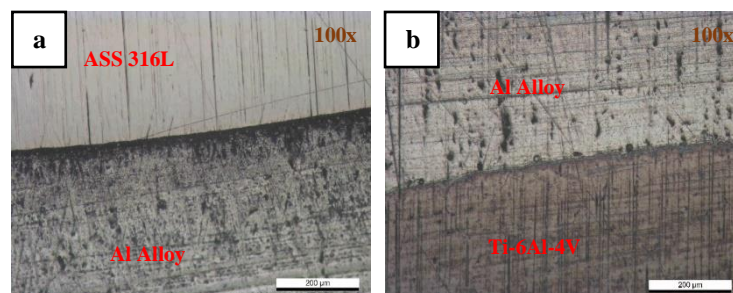


Figure 4.7: Microstructure for SWS-1



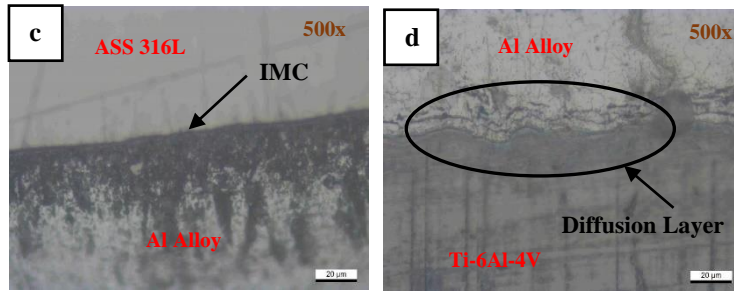


Figure 4.8: Microstructure for SWS-2

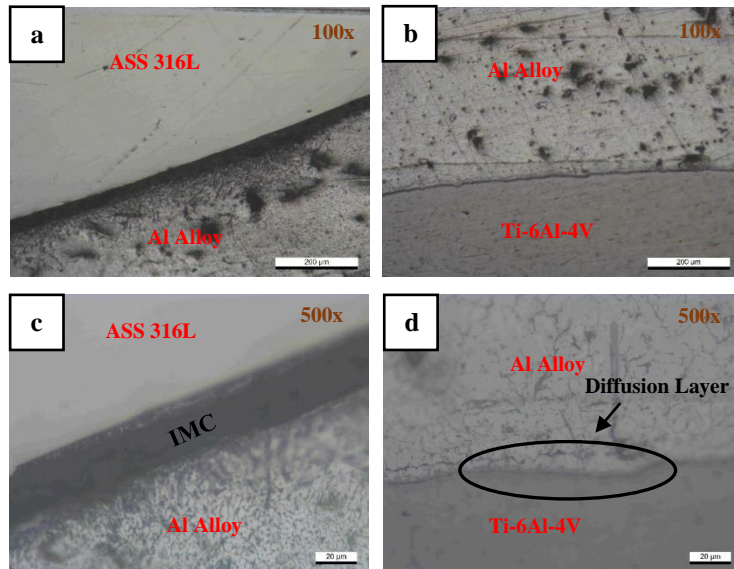


Figure 4.9: Microstructure for SWS-3

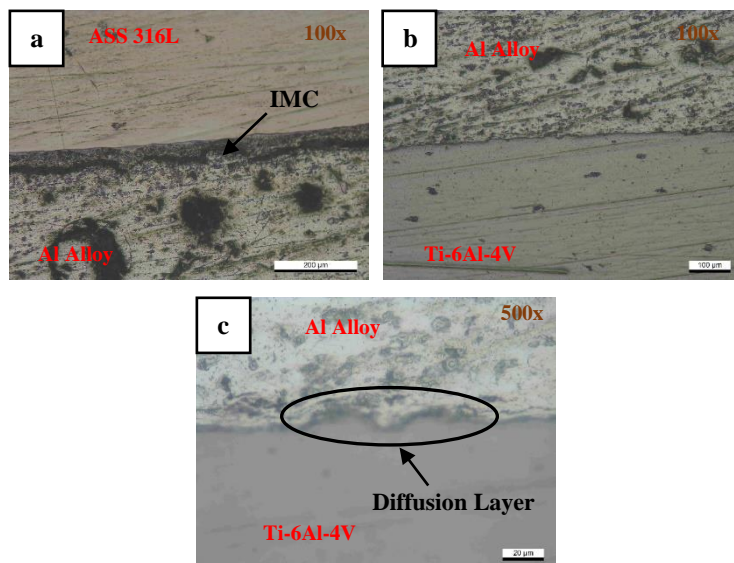


Figure 4.10: Microstructure for SWS-4

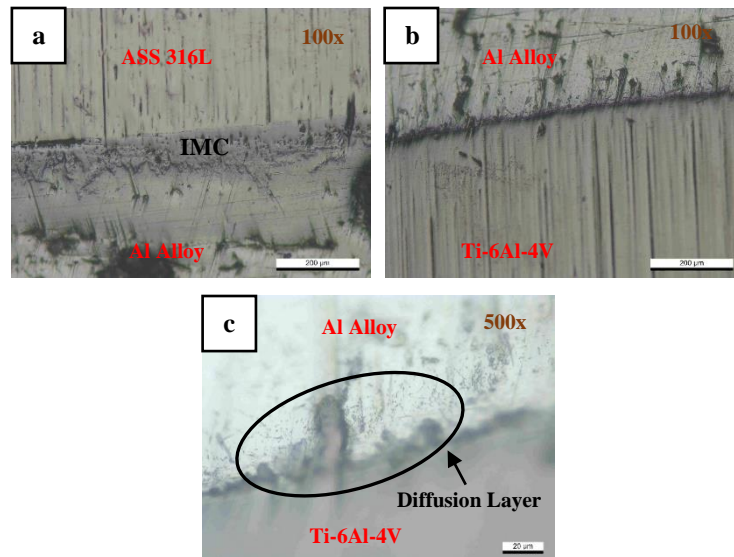


Figure 4.11: Microstruture for SWS-5

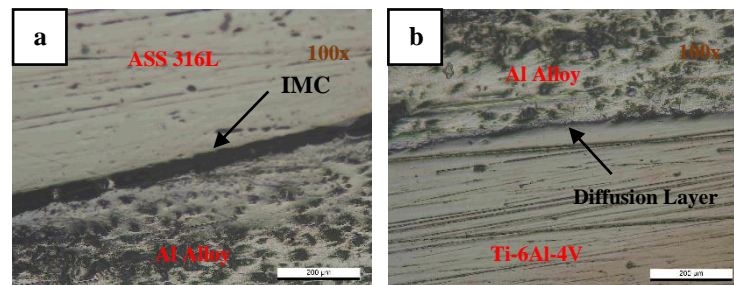


Figure 4.12: Microstructure for SWS-6

Figure 4.10a shows the optical image near ASS316L/Al interface with magnification of 100x. A thin flat layer formed at ASS316L side and morphology of serrate formed at Al alloy side (Tu & Qiu & Shi & Zhang & Zhang, 2011). Joining of ASS316L and Al alloy cause the formation of intermetallic compounds (IMC's), which are $FeAl_3$ and Fe_2Al_5 at interface (Tu & Qiu & Shi & Zhang & Zhang, 2011).

The thickness of IMC is the main factor affect the properties of ASS316L/Al joint. IMC can be defined as metallurgically bonding between ASS316L and Al alloy. Increasing in thickness of IMC at interface, decrease the joint strength of weld (Wan & Huang, 2018). Also, creation of IMC at Al/Fe interface lead to brittleness and pores formation due to different material's thermal conductivity (Das & Das & Paul, 2020). As can be seen in Figure 4.10a, IMC layer formed is thinner than the IMC layer at Figure 4.9a. Thus, there is the reason why the tensile strength of SWS-4 is higher than SWS-3. Similar go to other specimens, thicker the IMC layer, easier the cracks to

initiate and propagate, then weld joint fracture easily by tensile test, which cause lower tensile strength value (Wan & Huang, 2018). Due to the formation of intermetallic compound, every specimen is fracture at ASS316L/Al interface instead of Ti-6Al-4V/Al region. From the image of microstructure, it shown that thickness of IMC layer between ASS316L and Al alloy affected the fracture point of welded joint.

At Figure 4.10b and Figure 4.10c, it shows the optical image near Ti-6Al-4V/Al interface with magnification of 100x and 500x. Diffusion reaction occurs near Ti-6Al-4V/Al because Ti-6Al-4V consists of 6% aluminium contents which can bond with Al alloy. Diffusion reaction layer can observe clearly under the optical microscope with magnification of 500x.

The diffusion bonding at Ti-6Al-4V/Al interface can be related to weld current and interlayer thickness. Higher the weld current, higher the thickness of interface layer (Rajakumar & Balasubramanian, 2016). However, too high of weld current will cause expulsion, which contribute to imperfection of welded joint of Ti-6Al-4V and Al alloy (Mansor & Yusof & Ariga & Miyashita, 2018). Hence, reduction in tensile strength occurred. In order to obtain good diffusion bonding of interface layer, optimum thickness of Ti-6Al-4V/Al interface is necessary to get the maximum value of tensile strength (Rajakumar & Balasubramanian, 2016). From the figure above, the diffusion layer in Figure 4.9d is narrow in thickness compared to Figure 4.10c. This is because the weld current of 13.3kN is too huge with low weld pressure of 0.30MPa, so the diffusion reaction is weak between Ti-Al-4V and Al alloy in specimen 3. Although least diffusion bonding reaction occurred in specimen 3, the Ti-6Al-4V/Al interface is much stronger than the ASS316L/Al interface (Cao & Qi & Song & Feng, 2014). Thus, based on the microstructure analysis, it shows that the requirements for diffusion bonding of Ti-6Al-4V/Al interface is highly related to weld current setting and thickness of interface layer.

As conclusion, SWS-1, SWS-3, and SWS-6 have thicker IMC layer at ASS316L/Al interface compared to SWS-2, SWS-4, and SWS-5. However, SWS-2, SWS-4, and SWS-5 have wide diffusion layer at Ti-6Al-4V/Al interface. Therefore, thicker the ASS316L/Al interface, lower the tensile strength of welded joint. Then, weld current and interface thickness are the main factors affect the physical and mechanical properties of Ti-6Al-4V/Al interface.

4.3 MICROHARDNESS TEST

Microhardness test is an approach to measure the penetration resistance of weld joint. The method given by this test is Vickers hardness test and the unit of hardness is in HV. The load applied in this experiment is 200gf and dwell time is 15 seconds. The Vickers hardness is determined by load over the surface area of diamond indentation. The 2 samples measured in hardness test is SWS-3 and SWS-4, because these samples have the lowest and highest tensile strength. Figure 4.13 shown the hardness measurement along cross section of weld for sample 3 and sample 4. The hardness distribution measured from stainless steel (ASS 316L), then across aluminium alloy and titanium alloy (Ti-6Al-4V) with 19 indentation points.

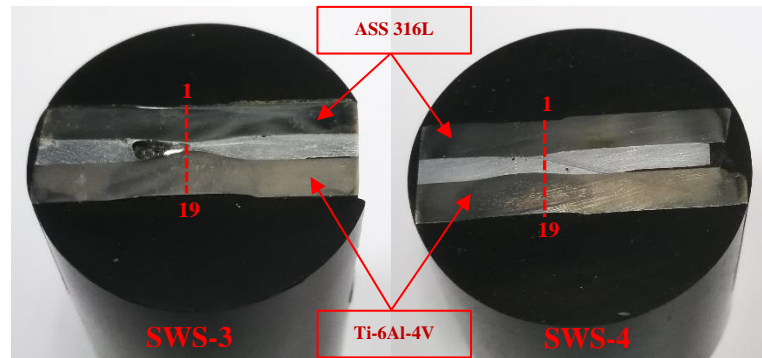


Figure 4.13: Hardness Distribution on Weld Geometry

The hardness measured along 3 regions which are base metal (BM), heat affected zone (HAZ), and transition layer (TL) as shown in Figure 4.14. There is no fusion zone at welding interface of each base metal (Tu & Qiu & Shi & Zhang & Zhang, 2011). In Table 4.2 and Table 4.3, it shown the microhardness results of specimen 3 and specimen 4. Then, Vickers microhardness distribution profile for both specimens are summarised in Figure 4.15 and Figure 4.16.

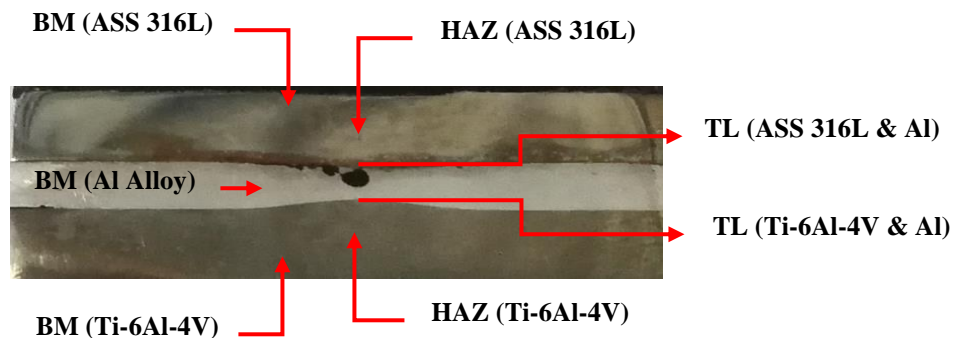


Figure 4.14: Structure of Weld Region

Table 4.2: Microhardness Results for SWS-3

No	Region	D1 (μm)	D2 (μm)	HV
1	BM (ASS 316L)	42.67	49.56	174.4
2		45.72	44.80	181.1
3		47.01	42.07	187.0
4	HAZ (ASS 316L)	41.83	41.74	212.4
5		42.32	42.31	207.1
6		42.30	42.39	206.8
7		42.82	42.79	202.4
8	TL (ASS 316L & Al)	63.18	56.79	103.1
9	BM (Al)	88.26	96.25	43.6
10		76.06	75.55	64.5
11		90.57	95.08	43.0
12	TL (Ti-6Al-4V & Al)	71.49	60.43	85.2
13	HAZ (Ti-6Al-4V)	32.18	31.56	365.1
14		32.28	31.65	363.0
15		31.46	31.29	376.8
16		31.60	31.46	373.1
17	BM (Ti-6Al-4V)	35.38	35.11	298.5
18		33.17	34.84	320.7
19		33.85	33.18	330.2

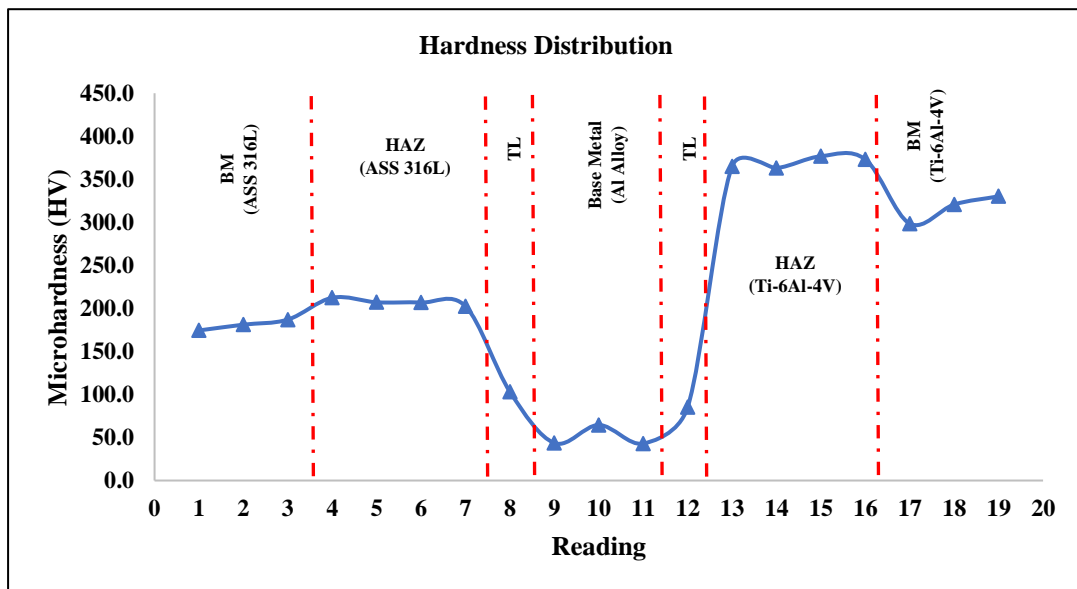


Figure 4.15.: Microhardness Distribution Profile for SWS-3

From Figure 4.15, the microhardness value shown slightly increase from base metal (BM) to heat affected zone (HAZ), then decrease drastically when approaching transition layer (TL). The average microhardness for heat affected zone (HAZ) of ASS

316L and Ti-6Al-4V is tested to be 207 and 370 HV respectively. The average microhardness for base metal of ASS 316L and Ti-6Al-4V is measured to be 181 and 316 HV respectively.

The microhardness of HAZ is higher than BM because presence of intermetallic compound (IMC). IMC can be defined as hard and brittle compound at weld joint. During welding, weld heat generated at heat affected zone make HAZ consists higher carbon percentage than BM because of the carburization process (Mansor & Yusof & Ariga & Miyashita, 2018). Based on the research, it shown that the carbon content in material is proportional to microhardness value. Thus, the region that undergo carburization process will experience higher carbon contents.

Table 4.3: Microhardness Results for SWS-4

No	Region	D1 (μm)	D2 (μm)	HV
1	BM (ASS 316L)	44.32	42.23	198.0
2		44.37	44.37	188.4
3		41.67	41.43	214.8
4	HAZ (ASS 316L)	41.02	41.00	220.5
5		39.95	39.94	232.4
6		39.09	39.73	238.8
7		40.79	40.15	226.4
8	TL (ASS 316L & Al)	77.07	70.34	68.3
9	BM (Al)	94.02	101.42	38.8
10		98.15	100.51	37.6
11		103.27	102.02	35.2
12	TL (Ti-6Al-4V & Al)	64.17	54.19	105.9
13	HAZ (Ti-6Al-4V)	28.88	31.48	407.2
14		30.68	30.61	394.9
15		30.54	30.48	398.4
16		31.70	31.64	369.7
17	BM (Ti-6Al-4V)	34.38	35.39	304.8
18		33.34	33.96	327.5
19		30.81	34.92	343.4

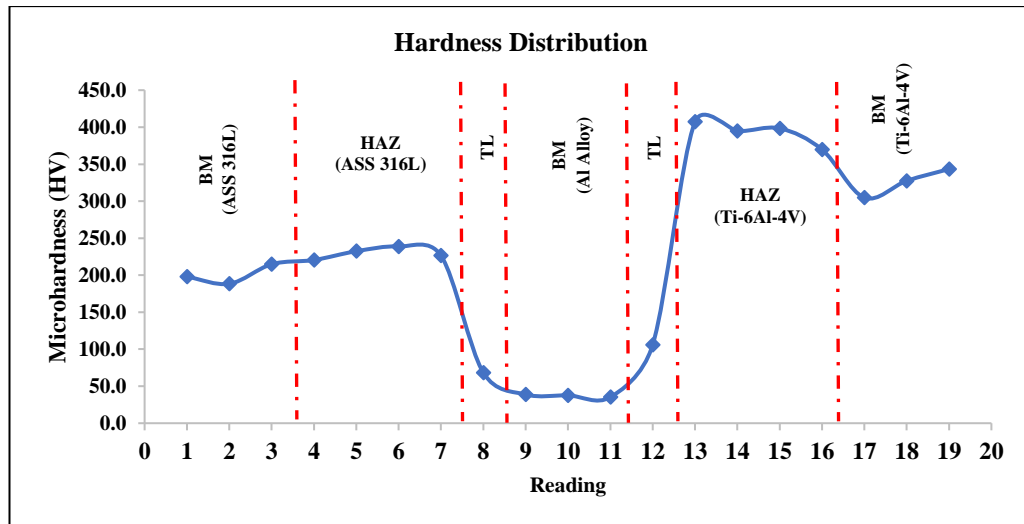


Figure 4.16: Microhardness Distribution Profile for SWS-4

Through the observation from Figure 4.16, the average microhardness of HAZ for ASS 316L and Ti-6Al-4V is 230 and 393 HV respectively. Then, the average microhardness of BM of ASS 316L and Ti-6Al-4V is 200 and 325 HV respectively.

The trend of microhardness profile in Figure 4.8 is obvious similar as Figure 4.7. However, the average microhardness of SWS-4 (good weld joint) is higher than SWS-3 (poor weld joint) because the nature of plasticity and strength of welded joint (Mansor & Yusof & Ariga & Miyashita, 2018). When the tensile strength obtained is increased, the microhardness value will increase.

As summary, there are different between SWS-3 and SWS-4 in term of microhardness. Higher the microhardness value, higher the strength of welded joint in one specimen. Through the observation from overall results, heat affected zone (HAZ) shown much harder and brittle than base metal (BM) after welding. As the results, the specimen undergoes brittle fracture at overlap area after the tensile test.

CHAPTER 5

CONCLUSION & RECOMMENDATIONS

5.1 CONCLUSION

In conclusion, the welding parameters which are weld current, weld pressure, and weld time (kept constant) have a direct impact on tensile strength, microstructure, and microhardness of specimens. For dissimilar metal sheets welding, weld current is the most significant welding parameters in resistance spot welding.

From the tensile strength experiment, increasing in weld current definite will increase the tensile strength of weld joint because growth up of weld nugget diameter. However, increase further weld current setting will cause reduction in tensile strength because occurrence of expulsion at heat affected zone (HAZ) may limit the growth size of weld nugget. Apart from this, increasing in electrode force also contributed to high weld strength. The reason is weld current will affect directly to weld pressure (electrode force) and inversely to weld time. So, high setting of weld current must be matched with high electrode force in order to achieve optimisation during welding. However, increase electrode force further will cut down the strength of weld joint. The reason behind the theory is extremely high of welding force will reduce the heat input, so it caused the weld nugget size decreased. Besides that, excessive indentation caused by electrodes tips on sheet surface cause high pressing force at faying region, thus it cut down weld strength (tensile strength) of specimen.

In microstructural analysis, the microstructure of ASS 316L/Al and Ti-6Al-4V/Al are display clearly in terms of image with magnification of 100x and 500x. From this study, thicker the ASS316L/Al interface, lower the tensile strength of welded joint. This is because ASS316/Al will form intermetallic compound (IMC), which is hard and brittle behaviour at welded joint. Then, weld current and interface

thickness are the main factors affect the physical and mechanical properties of Ti-6Al-4V/Al interface. Optimum in weld current and critical in interface thickness are necessary for diffusion bonding between Ti-6Al-4V and Al alloy.

Moreover, the microhardness is directly proportional to the tensile strength of specimens. From this study, the heat affected zone (HAZ) shows higher microhardness value compared to base metal (BM) region. Due to existence of intermetallic compound (IMC) and high percentage of carbon content, it formed a hard phase at HAZ. Then, the microhardness value will increase when the tensile strength increased due to the nature of plasticity and strength of welded joint. Lastly, the highest microhardness of weld joint is at heat affected zone of Ti-6Al-4V followed by heat affected zone of ASS316L.

5.2 RECOMMENDATIONS

The purpose of this study mainly is to evaluate the impact of welding parameters on tensile strength, microstructure, and microhardness. Basically, the welding parameters must be modified when there are variety in material types and thickness. Thus, performance of welding parameters must be tested from time to time in order to achieve optimum condition during welding. Therefore, the suggestions below are considered for future improvement in spot welding.

- a) Prepare more specimens with various welding parameters to increase the accuracy and consistency of results. This is because more specimens will reduce the error in interpreting data and information.
- b) Non-destructive test is preferred instead of destructive test. This is because non-destructive test applied at tensile test will cut down the time spent in data collection. With the aid of simulation, it will get faster and more accurate result compared to machine.
- c) The thickness of specimens should be reduced within 1 mm and 2 mm. This is because higher the thickness of material, the weld current required will be increased. Thus, it will cause a high potential of spark during welding.

REFERENCES

- Ahmed, Y. M., Sahari, K. S. M., Ishak, M., & Khidhir, B. A. (2014). Titanium and its alloy. *International Journal of Science and Research*, 3(10), 1351-1361.
- Asari, R. (2018). *Resistance Spot Welding - Impact of Process Parameters on Weld Nugget Formation*.
- Bharath, P., & Sridhar, V. (2014). Optimization of 316 stainless steel weld joint characteristics using Taguchi technique. *Procedia Engineering*, 97, 881-891.
- Cao, J., Qi, J., Song, X., & Feng, J. (2014). Welding and joining of titanium aluminides. *Materials*, 7(7), 4930-4962.
- Casalino, G., Facchini, F., Mortello, M., & Mummolo, G. (2016). ANN modelling to optimize manufacturing processes: The case of laser welding. *IFAC-PapersOnLine*, 49(12), 378-383.
- Das, T., Das, R., & Paul, J. (2020). Resistance spot welding of dissimilar AISI-1008 steel/Al-1100 alloy lap joints with a graphene interlayer. *Journal of Manufacturing Processes*, 53, 260-274.
- Ertek Emre, H., & Kaçar, R. (2016). Resistance Spot Weldability of Galvanize Coated and Uncoated TRIP Steels. *Metals*, 6(12). doi:10.3390/met6120299
- Faiyaz, S., & Borke, J. G. (2017). The Experimental Investigation and Analysis of Spot Welding Process Parameters for Maximum Tensile Strength. *International Journal of Advance Research, Ideas and Innovations in Technology*, 3(3) www.IJARIT.com.
- Gawai, B., & Sedani, C. (2016). Optimization of Process Parameters for Resistance Spot Welding Process of HR E-34 Using Response Surface Method–A Review. *International Journal of Science and Research (IJSR)*, 5, 2002-2008.
- Hou, L., Qiu, R., Cui, L., Shen, Z., & Li, Q. (2015). *Microstructure and mechanical property of resistance spot welded joint between pure titanium and stainless steel with interlayer of Nb*. Paper presented at the 5th International Conference on Advanced Design and Manufacturing Engineering.

- Kahraman, N. (2007). The influence of welding parameters on the joint strength of resistance spot-welded titanium sheets. *Materials & Design*, 28(2), 420-427.
- Kianersi, D., Mostafaei, A., & Amadeh, A. A. (2014). Resistance spot welding joints of AISI 316L austenitic stainless steel sheets: Phase transformations, mechanical properties and microstructure characterizations. *Materials & Design*, 61, 251-263.
- Li, K., Xue, H., Zhao, K., Wang, S., Wang, T., & Song, R. H. (2019). *Determination of Ratio of Yield Strength and Reduced Modulus during Cold Work Processing in 304 Austenitic Stainless Steel*. Paper presented at the Key Engineering Materials.
- Mansor, M. S. M., Yusof, F., Ariga, T., & Miyashita, Y. (2018). Microstructure and mechanical properties of micro-resistance spot welding between stainless steel 316L and Ti-6Al-4V. *The International Journal of Advanced Manufacturing Technology*, 96(5-8), 2567-2581.
- Mercan, E., Ayan, Y., & Kahraman, N. (2019). Investigation on joint properties of AA5754 and AA6013 dissimilar aluminum alloys welded using automatic GMAW. *Engineering Science and Technology, an International Journal*.
- Mishra, S. S. Research on Resistance Spot Welding of Dissimilar Metal Sheets: An Overview. "Technological Advancement in Manufacturing & Processing of New Materials" (TAMPNM-2016) 9th–10th April 2016, 35.
- Mittal, R., Gupta, A., Pratap, K., Shukla, P., & Gupta, S. (2020). Microstructural and mechanical behavior in dissimilar T91/T22 welded pipes. *Materials today: proceedings*.
- Nasir, Z., & Khan, D. M. (2016). Resistance spot welding and Optimisation techniques used to optimise its process parameters. *International Research Journal of Engineering and Technology (IRJET)*, 3(5), 887-893.
- Petrík, J., Blaško, P., Ďurišin, J., Vasilňáková, A., & Guzanová, A. (2019). THE ORIENTATION OF THE GRAINS AND INDENTATION SIZE EFFECT. *Annals of the Faculty of Engineering Hunedoara*, 17(3), 69-72.
- Petrík, J., & Palfy, P. (2011). The Influence of the Load on the Hardness. *Metrology and measurement systems*, 18(2), 223-234.

- Rajakumar, S., & Balasubramanian, V. (2016). Diffusion bonding of titanium and AA 7075 aluminum alloy dissimilar joints—process modeling and optimization using desirability approach. *The International Journal of Advanced Manufacturing Technology*, 86(1-4), 1095-1112.
- Raut, M., & Achwal, V. (2014). Optimization of spot welding process parameters for maximum tensile strength. *International Journal of Mechanical Engineering and Robotics Research*, 3(4), 507-517.
- Rawal, M. R., & Inamdar, K. (2014). Review on various optimization techniques used for process parameters of resistance spot welding. *International Journal of Current Engineering and Technology*, 3, 160-164.
- Shamsul, J., & Hisyam, M. (2007). Study of spot welding of austenitic stainless steel type 304. *Journal of Applied Sciences Research*, 3(11), 1494-1499.
- Shelly, K., & Sahota, D (2017). A Review Paper on Resistance Spot Welding of Austenitic Stainless Steel 316. *International Journal of Engineering Trends and Technology (IJETT)*, 47(7), 424-429.
- Singh, P., Pungotra, H., & Kalsi, N. S. (2017). On the characteristics of titanium alloys for the aircraft applications. *Materials today: proceedings*, 4(8), 8971-8982.
- Tu, Y. M., Qiu, R. F., Shi, H. X., Zhang, X., & Zhang, K. K. (2011). *Resistance spot welding between titanium and stainless steel with an aluminum alloy insert*. Paper presented at the Advanced Materials Research.
- Wang, Y., Tao, W., & Yang, S. (2019). A Method for Improving Joint Strength of Resistance Spot Welds of AA 5182-O Aluminum Alloy. *Journal of Manufacturing Processes*, 45, 661-669.
doi:<https://doi.org/10.1016/j.jmapro.2019.07.024>
- Wan, L., & Huang, Y. (2018). Friction stir welding of dissimilar aluminum alloys and steels: a review. *The International Journal of Advanced Manufacturing Technology*, 99(5-8), 1781-1811.
- Yu, Z. (2018). Review of Ti to Steel Dissimilar Joining. *Research & Development in Material Science*, 5(5). doi:10.31031/rdms.2018.05.000623

Zhang, X., Zhang, J., Chen, F., Yang, Z., & He, J. (2017). Characteristics of resistance spot welded Ti6Al4V titanium alloy sheets. *Metals*, 7(10), 424.

Zhou, K., & Yao, P. (2019). Overview of recent advances of process analysis and quality control in resistance spot welding. *Mechanical Systems and Signal Processing*, 124, 170-198. doi:<https://doi.org/10.1016/j.ymssp.2019.01.041>